

Two-Stage Grid-Connected PV System With Reserve Power Control Strategy

Thayyuru Himagiri^{1*}, B. Subba Reddy², R. Maheswar Reddy³
 PG student¹, Assistant Professor², Assistant Professor³, Department of EEE,
 Sree Vidyanikethan Engineering College, Tirupati, AP, India

Abstract : The still increasing penetration of grid connected photovoltaic (PV) systems, advanced active power control functionalities have been introduced. A reserve power control, where namely the active power from the PV panels is reserved during operation, is required for grid support. A cost-effective solution to realize the reserve power with two-stage grid-connected PV systems is proposed. The proposed solution routinely employs a maximum power point tracking control to estimate the available PV power and a constant power generation (CPG) control to achieve the reserve power. In this method, the solar irradiance and temperature measurements that have been used in conventional reserve power control schemes to estimate the available PV power are not required, and thereby, being a sensor less approach with reduced cost. At the grid side, the stored energy in the DC link is adaptively controlled to minimize the power fluctuation during the available PV power estimation process, where the excessed energy is temporarily stored in the DC link. Have been performed on a 3-kW two-stage single-phase grid-connected PV system.

Index Terms—Active power control, constant power generation (CPG) control, grid-connected power converters, maximum power point tracking (MPPT), reserve power control (RPC), photovoltaic (PV) systems.

1. INTRODUCTION

In recent decades, the penetration level of photovoltaic (PV) systems has been continuously increasing, especially for grid-connected applications [6]-[10]. Several advanced active power control strategies have been defined [4]-[9], where the PV system is expected to be more active in the power network beyond a purely power-generating unit. One of the advanced functionalities in grid-connected PV systems is to reserve active power for potential grid voltage or frequency regulations [9], [2]-[9], where a certain amount of active power is reserved during operation. The reserve power control (RPC) can be adopted for potential frequency regulation during a short period [6]-[16]. Energy storage devices are normally employed to realize the reserve power in PV systems [11]-[16]. However, high cost and limited lifetime are the two main drawbacks, which makes this solution not so cost effective, and also becoming the main driving forces for advanced control solutions with reduced cost and complexity [10]. In order to do so, the modified maximum power point tracking (MPPT) algorithm has to be able to regulate the PV power P_{pv} at a certain power limit P_{limit} , as it has been proposed in [5]-[17]. To achieve the RPC strategy, The set-point P_{limit} has to be calculated by subtracting the available PV power P_{avai} with the required amount of reserve power ΔP as

$$P_{pv} = P_{limit} = P_{avai} - \Delta P \quad (1)$$

In light of the aforementioned issues, it calls for a cost effective and simple solution to realize the RPC strategy. The proposed reserve power control (RPC) strategy to fill out this gap, where the solar irradiance measurements are not required for the available PV power estimation. The proposed solution routinely employs the MPPT operation to measure the available PV output power, which is simple and more generic [29]. Then, the PV output power is regulated according to the required amount of the reserve power by means of a constant power generation (CPG) strategy [12],[13]. At the grid-side converter, the stored energy in the DC-link is also adaptively controlled to buffer the PV power increase during the MPPT operation, and thereby, keep the injected AC power to follow the required reserve power profile. The proposed approach can overcome the limitation in [30], where the RPC constraint cannot be maintained during the MPPT operation.

2. SYSTEM DESCRIPTION OF TWO-STAGE PV SYSTEMS

The system configuration of a two-stage grid-connected PV systems is shown in Fig. 1. This two-stage configuration is widely used in the residential/commercial PV systems [21], [22], where it consists of two power converters: 1) the PV-side DC-DC boost converter and 2) the grid-side DC-AC inverter. Basically, the boost converter is responsible for extracting the PV power P_{pv} , which is achieved by regulating the PV voltage V_{pv} at the corresponding operating point in the power-voltage ($P-V$) the V_{MPP} for the MPPT operation. Then, the grid-side converter, which is realized by a full-bridge topology, delivers the extracted PV power to the AC grid by regulating the DC-link voltage V_{DC} to be constant through the control of the grid current. In this case, a bipolar pulse width modulation technique is used in order to eliminate the common-mode voltage, and thus, minimize the leakage current [24]. This is a common requirement for transformer less PV applications. In addition, the grid-side converter also requires a proper synchronization of the injected current with the grid voltage by means of phase-locked loops, and ensures the power quality of the injected grid-current with harmonic compensators being implemented.

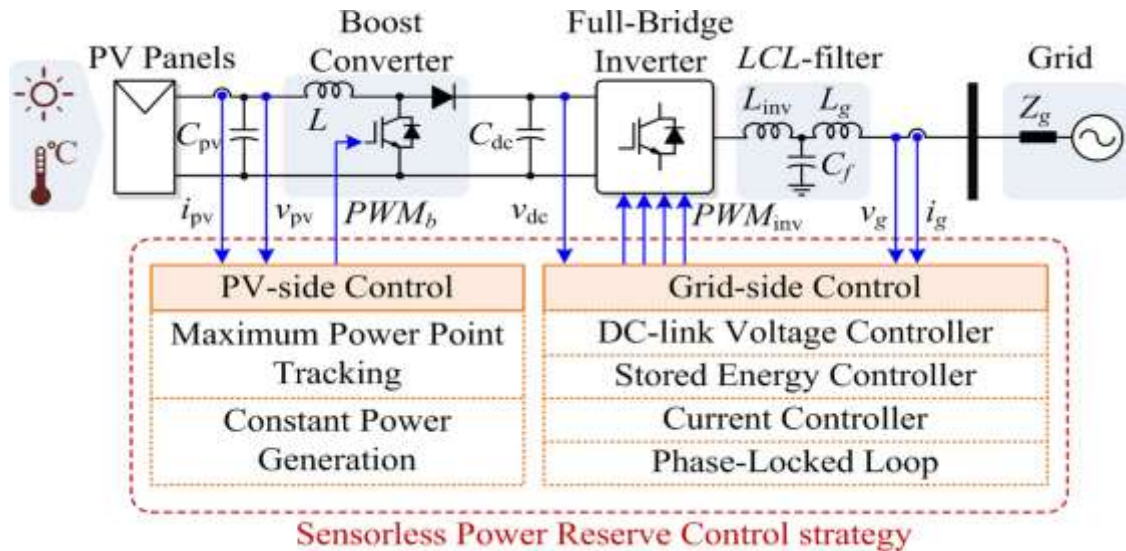


Fig. 1 System configuration and control structure of a two-stage grid connected PV system with the RPC strategy

In fact, the DC and AC power are decoupled in the two-stage configuration, where the DC-link capacitor acts as an energy buffer to decouple the DC and AC power. Thus, it is possible to adaptively adjust the stored energy in the DC-link to some extent during operation. In that case, the dc-link voltage is not always kept as constant in order to temporarily reserve the extracted power from the PV, which is the main idea of the proposed RPC strategy and will be further discussed in details in the following.

3. PROPOSED SENSORLESS RESERVE POWER CONTROL STRATEGY

3.1. Operational Principle

The proposed RPC strategy is a combination of two operational modes: MPPT and CPG, which are employed for different control objectives. The main purpose of the MPPT operation is to estimate the available PV power. When the operating point of the PV arrays is regulated at the MPP, the available power of the PV arrays P_{avail} can be estimated from the measured PV output power P_{pv} . By routinely assigning the MPPT operation, the available power can continuously be estimated during operation. In fact, this concept is similar to the “sample and hold (S&H)” process in digital control. Once the available PV power is estimated with the MPPT operation, the set point of the CPG operation P_{limit} can be calculated according to for a given amount of reserve power ΔP . Accordingly, the RPC strategy employs the CPG operation to regulate the PV power in order to provide a power reserve as demanded. The corresponding extracted PV power from the DC-DC boost converter with the combination of MPPT and CPG modes. In order to ensure that the power injected to the AC grid always follows the demand in the case of the RPC. Reserve power requirement in the Danish grid code, where ΔP is the amount of reserve power level, the peak power during the MPPT mode should be buffered. In the proposed approach, the DC-link voltage is increased during this period to temporarily store the excessed energy due to the peak power injection. In this regard, the proposed solution can be flexibly adapted to any two-stage PV system configuration, where the PV- and the grid-side converters can be controlled independently. The control algorithm of the PV-side boost converter and grid-side converter to achieve the discussed strategy is presented in the following.

3.2. Control Algorithm of the PV-Side Boost Converter

As discussed previously, there are two operating modes for the boost converter. Namely, the MPPT operation is employed to estimate the available PV power, and the CPG control is employed to regulate the PV output power to follow the reserve power demand. That is to say, in the case of RPC operation, the ambient temperature is assumed to be constant. With the aforementioned MPPT operation, the available PV power can be estimated by simply measuring the PV power during the steady-state MPPT periods. Once the APE process is done, the PV system enters into the CPG mode where the operating point of the PV systems has to be regulated below the MPP in order to achieve $P_{pv} = P_{limit}$ (and thus, the reserve power). It can be seen from the P-V characteristic of the PV panel. That there are two possible operating points for a certain level of P_{limit} and irradiance level. However, it should be aware that the operating point at the right side of the MPP can introduce instability during a fast irradiance drop. In that case, the open-circuit voltage of the PV panels V_{oc} decreases as the irradiance level drops, and the operating point may fall into (and stay at) the open-circuit condition. Under this situation, the CPG operation becomes unstable and the PV system will not able to deliver any power from the PV panel to the grid, as it has been demonstrated. With this concern, the operating point of the PV system is perturbed to the left side of the MPP during the CPG operation, as it is also illustrated in [12]-[14]. The reference PV voltage v_{pv}^* during the CPG mode can be summarized as

$$v_{pv}^* = \begin{cases} v_{MPPT} & \text{When } P_{pv} \leq P_{limit} \\ v_{pv} - v_{step} & \text{When } P_{pv} > P_{limit} \end{cases} \quad (2)$$

where v_{MPPT} is the reference voltage from the MPPT algorithm and v_{step} is the perturbation step size. Notably, the reference v_{MPPT} has nothing to do with the previous CV-MPPT algorithm (which is only used during the APE process), but the v_{MPPT} is needed during the CPG operating mode in order to keep the operating point of the PV system at $P_{pv}=P_{limit}$. This is due to the fact that the PV power may not be kept exactly at the P_{limit} in practice, but it will oscillate around that operating point with minimum deviations. In that case, the PV voltage needs to follow the reference from the P&O MPPT algorithm when $P_{pv} \leq P_{limit}$, in order to move the operating point back close to $P_{pv}=P_{limit}$. Further discussions about CPG algorithms can be found in [10]. The control structure of the PV-side boost converter is shown in Fig. 2, where a proportional-integral (PI) controller is employed to regulate the PV voltage v_{pv} according to its reference v_{pv}^* . To avoid any confusion, due to the two operating modes, the reference voltage v_{pv}^* in Fig. 2 is obtained from during the APE process (MPPT operation), while the reference voltage is employed only during the CPG mode. In both cases, the control structure remains the same, while only the reference PV voltage v_{pv}^* is changed, as shown in Fig. 2.

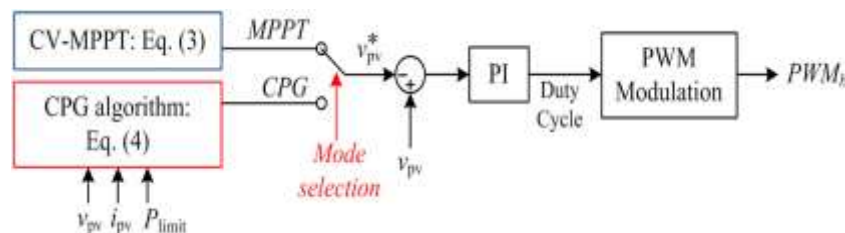


Fig. 2 Control scheme of the PV-side boost converter with the MPPT and CPG operation

3.3. Control Algorithm of the Grid-Side Converter

Regardless of the operating mode of the PV-side boost converter, the objective of the grid-side converter is to always keep the injected AC power to follow the RPC constraint as

$$\langle P_{ac} \rangle = P_{limit} = P_{avail} - \Delta P, \tag{3}$$

with $\langle P_{ac} \rangle$ being the average injected AC power, P_{limit} being then set-point (reference), P_{avail} being the available PV power, and ΔP being the required amount of reserved power. In order to do so, the peak power during the APE period has to be temporarily stored in the DC link. Following, the control scheme of the grid-side converter in Fig. 3 is employed, where a stored energy controller is plugged into the typical DC-link voltage controller for calculating the reference grid current. Basically, the DC-link voltage controller will give an amplitude reference of the grid current $|i_g^*|$ which keeps the DC-link voltage v_{dc} constant and delivers all the extracted PV power to the AC grid (which is the case during the CPG mode). However, if the average injected ac power $\langle P_{ac} \rangle$ exceeds the power limit P_{limit} , and measured DC-link voltage, $\langle P_{ac} \rangle$ is the average injected AC power, and P_{limit} is the set point. A certain amount of current Δi_g corresponding to $k_{ac}(\langle P_{ac} \rangle - P_{limit})$ is subtracted from the reference $|i_g^*|$ by the stored energy controller. The proportional gain k_{ac} should be selected as $\sqrt{2}/V_g$ (with a small adjustment in practice to compensate power losses in the DC-link, e.g., parasitic resistance in the DC-link capacitor), where V_g is the RMS value of the grid voltage. In this way, the amount of the grid current reduction Δi_g , which will allow the power difference $(\langle P_{ac} \rangle - P_{limit})$ be stored in the DC-link, can be determined. Consequently, the actual DC-link voltage v_{dc} will be higher than the reference v_{dc}^* during the MPPT mode, but the peak power will not propagate to the AC grid. In this approach, the stored energy in the DC-link is controlled indirectly through the compensation of the grid current, which offers a faster and more effective response than the solution by directly calculating the corresponding DC-link voltage. This is due to the typical limited bandwidth of the DC-link voltage controller. Notably, v_{dc} should also be within a certain range for single-phase grid-connected inverters systems, in order to ensure the power delivery to the grid and safety. Thus, there is a certain limit of the amount of reserved power ΔP in order to ensure that the DC-link voltage will not reach the system maximum voltage limit [32], [33], which will be discussed in above sections.

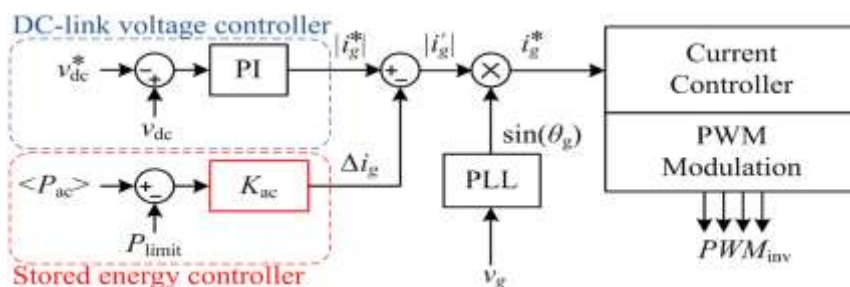


Fig. 3 Control scheme of the grid-side converter with the DC-link voltage controller and the stored energy controller

4. DESIGN CONSIDERATION OF THE RPC STRATEGIES

In order to achieve a high control performance using the RPC strategy, several design considerations should be discussed to assist the practical implementations.

4.1. Improving the Reserve Power Accuracy by Compensating Inverter Power Losses

So far, the efficiency of the converters are not considered. In other words, it is assumed that the PV power P_{pv} is equal to the injected AC power $\langle P_{ac} \rangle$ during the CPG operation. However, there are power losses in the power converters, especially from the power devices during the switching and conduction, which reduces the converter efficiency. The power losses cannot be neglected and should be compensated, in order to achieve a high-accuracy operation. Tracking the efficiency of the power converter into account, the power injected to the grid from the PV arrays becomes where η is the efficiency of the power converter.

$$\langle P_{ac} \rangle = \eta \cdot P_{pv} \quad (4)$$

$$P_{pv} - \langle P_{ac} \rangle = (1 - \eta) \cdot P_{pv} \quad (5)$$

It can be observed in that there is always a certain amount of power losses from the PV side to the grid side corresponding to $(1 - \eta) \cdot P_{pv}$. Power extraction from the PV arrays according to the RPC strategy with the power loss compensation, where t_{res} is the time response during the operating mode transition, f_{APE} is the sampling rate of the available PV power estimation process, and η is the efficiency of the power converter. In order to maintain the reserve power constraint with respect to the injected AC power, the amount $(1 - \eta) \cdot P_{pv}$ should be subtracted from the reference ΔP when calculating the power limit as

$$P'_{limit} = P_{avai} - [\Delta P - (1 - \eta) \cdot P_{pv}] \quad (6)$$

Where P'_{limit} is the compensated power limit. By replacing the P_{limit} with P'_{limit} at the PV-side controller in, the power losses in the power converter are compensated, as it is illustrated.

4.2. Minimizing the Excessed Energy With Fast CPG Algorithms During Transients

The key performance of the RPC strategy is a fast operation during the APE process in order to minimize the excessed energy in the DC-link. There are two intermediate steps during this period: 1) CPG to MPPT (during t_1) and 2) MPPT to CPG (during t_2) transitions, where a certain time response t_{res} is required. With the CV-MPPT method discussed above sections, the CPG to MPPT transition can be achieved very fast, where the reference $v^* = K_{OC} V_{OC}$ is directly assigned. Thus, the remaining issue is to ensure a fast transient response of the CPG algorithm during the MPPT to CPG transition. A simple and effective solution is to directly apply the last operating point during the steady-state CPG operation as a reference PV voltage once the APE process is done. In this way, the operating point of the PV can move back relatively fast to the previous operating point in the CPG mode within one sampling period. After that, the CPG algorithm is employed in steady-state CPG operation (during t_3). With this approach, Power extraction from the PV arrays according to the RPC strategy with the previous operating point during the CPG mode being applied after the available PV power estimation process, where t_{res} is the time response during the operating mode transition, f_{APE} is the sampling rate of the available PV power estimation process, and η is the efficiency of the power converter.

The time response during the transition t_{res} is minimized, as it can be compared from t_{res} . (with normal CPG algorithm, where a number of sampling during MPPT to CPG transition is required) and (with fast CPG algorithm). This solution is effective when the sampling rate of the APE process is much faster than the solar irradiance fluctuation, which is usually the case for the PV system in practice. Under this condition, it can be assumed that the operating point during the CPG mode for each sampling changes relatively slow, due to the high sampling rate of APE.

4.3. Maximum Amount of the Reserve power

The maximum amount of reserve power ΔP_{max} is limited by the stored energy capacity of the DC-link capacitor. This is due to the fact that during each APE process, the excessed energy will be injected into the DC link, which has a limited energy capacity. According to the excessed energy during the APE process ΔE can be approximated as

$$\Delta E = \frac{1}{2} (\Delta P - (1 - \eta) \cdot P_{pv}) t_{res} \quad (7)$$

$$\Delta E = \frac{1}{2} (P_{avai} - P'_{limit}) t_{res} \quad (8)$$

When this excessed energy is stored in the DC link, it will cause the DC-link voltage V_{dc} increase according to

$$\Delta E = \frac{1}{2} C_{dc} (v_{dc,1}^2 - v_{dc,0}^2) \quad (9)$$

Where $v_{dc,0}$ is the initial DC-link voltage, which corresponds to the reference DC-link voltage v_{dc}^* in the RPC strategy $v_{dc,t}$, t is the peak value of the dc-link voltage, which is limited by the maximum allowable dc-link voltage $v_{dc,max}$ according to the grid regulations. Thus, the maximum excessed energy that can be stored in the DC-link during each APE process is determined as follows:

$$\Delta E_{max} = \frac{1}{2} C_{dc} (v_{dc,max}^2 - v_{dc}^{*2}) \tag{10}$$

According to ,the maximum amount of the reservpower ΔP_{max} is obtained as

$$\Delta E = \frac{C_{dc}}{t_{res}} (v_{dc,1}^2 - v_{dc,0}^2) + (1 - \eta) \cdot P_{pv} \tag{11}$$

$$\Delta E_{max} = \frac{C_{dc}}{t_{res}} C_{dc} (v_{dc,max}^2 - v_{dc}^{*2}) + (1 - \eta) \cdot P_{pv}. \tag{12}$$

It is noticed from that, in order to increase ΔP_{max} , either a large DC-link capacitor C_{dc} is needed or the time response t_{res} has to be minimized. However, increasing the DC-link capacitance is usually not preferable considering the cost, size, and reliability of the system. The DC-link capacitance C_{dc} is designed based on the maximum ripple voltage Δv requirement during normal operation, where the DC-link capacitance is determined by

$$C_{dc} = \frac{P_{pv}}{(2\pi f_g) \Delta v \cdot v_{dc}} \tag{13}$$

At the rated power, the DC-link voltage is regulated at 450 ± 5 V. Thus, the required DC-link capacitance is around 2.2 mF according. Notably, this is a typical design for single-phase inverter, where the dc-link voltage inevitably contains the double-line frequency ripples during operation. This DC-link capacitor, however, can be used to store the excessive energy in the RPC operation. In other words, the DC-link capacitor is not oversized or specifically designed for the reserve power purpose. Consequently, from this standpoint, reducing the time response t_{res} is a more viable solution to maximize the reserve power of a predesigned two-stage PV system.

4.4. Maximum Sampling Frequency of the APE Process

The accuracy of the APE relies on its sampling frequency f_{APE} . In general, the accuracy of the APE increases as its sampling rate f_{APE} increases, especially during the changing irradiance condition. However, the constraint that limits the sampling frequency f_{APE} is the required response time by the DC-link voltage controller in order to reach the steady state after the peak power injection due to the APE process. Specifically, the DC-link voltage has to be discharged to its nominal value at the end of each APE sampling. Otherwise, if the excessed energy is injected to the DC-link during the discharging period, the DC-link voltage will oscillate. This will lead to an unstable operation, since the boost converter can no longer regulate its input voltage when the output voltage is oscillating significantly, as it will be exemplified later via experiments. The variation in the DC-link voltage v_{dc} during each APE process is illustrated in Fig. 3.8. At the beginning of each APE process, the DC-link voltage will reach its peak value after $t = t_{res}$, which is the time duration where the excessed energy is injected into the DC link. After that, the DC-link voltage will be slowly discharged by the DC-link voltage controller. During this period, the stored energy controller is deactivated, since $(P_{ac} - P_{limit}) = 0$. Thus, the required discharging time t_{dc} corresponds to the settling time of the DC-link voltage controller, and the maximum sampling frequency of the APE process $f_{APE,max}$ can be obtained as

$$f_{APE,max} = \frac{1}{t_{res} + t_{dc}} \tag{14}$$

5.PERFORMANCE VERIFICATION OF THE PROPOSED RPC STRATEGIES

In order to verify the effectiveness of the proposed RPC strategy, the tests have been carried out with the shown in Fig. 4. It should be pointed out that an LC filter is used, and connected to the grid through an isolation transformer. Together with the leakage inductance of the isolation transformer, an LCL-filter is formed. At the PV-side, a PV simulator has been adopted. The control algorithms have been implemented in an FPGA system.

5.1. SIMULINK MODELING AND RESULTS O RPC CONTROL STRATEGY

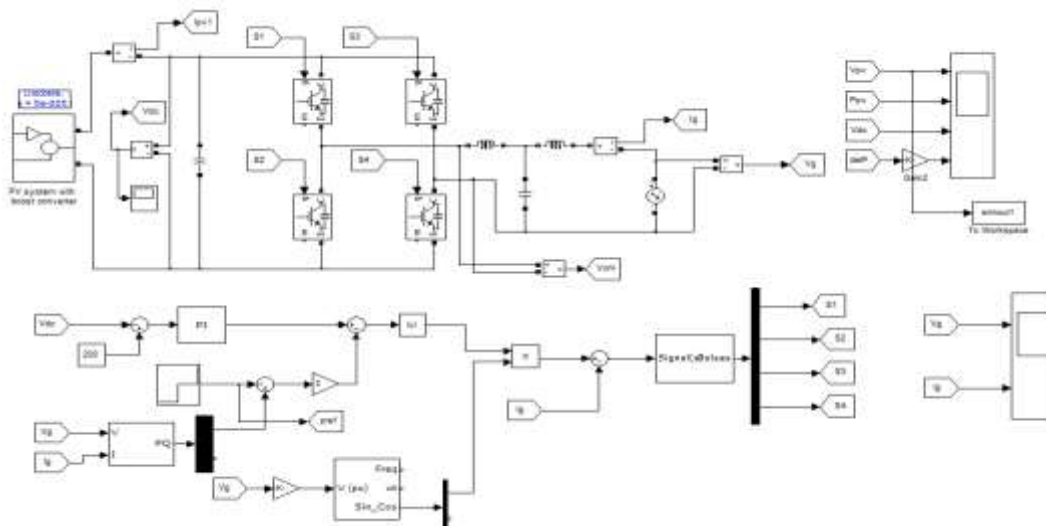


Fig. 4 Simulink modeling of with RPC control strategy

The Fig.4 represents Simulink modeling of with RPC control strategy over all operation is generation of solar energy from light energy, then it converts electrical energy which is DC output. The P&O algorithm is used to estimate the available PV output power. The PV output power is given to the boost converter, boost up the PV power otherwise the boost up energy is stored in to battery. Used in full bridge inverter DC energy is converted in to AC inverter output is filtering and connected to grid. The whole operation is controlled in to the control strategy is Constant Power Generation (CPG).

RESULTS

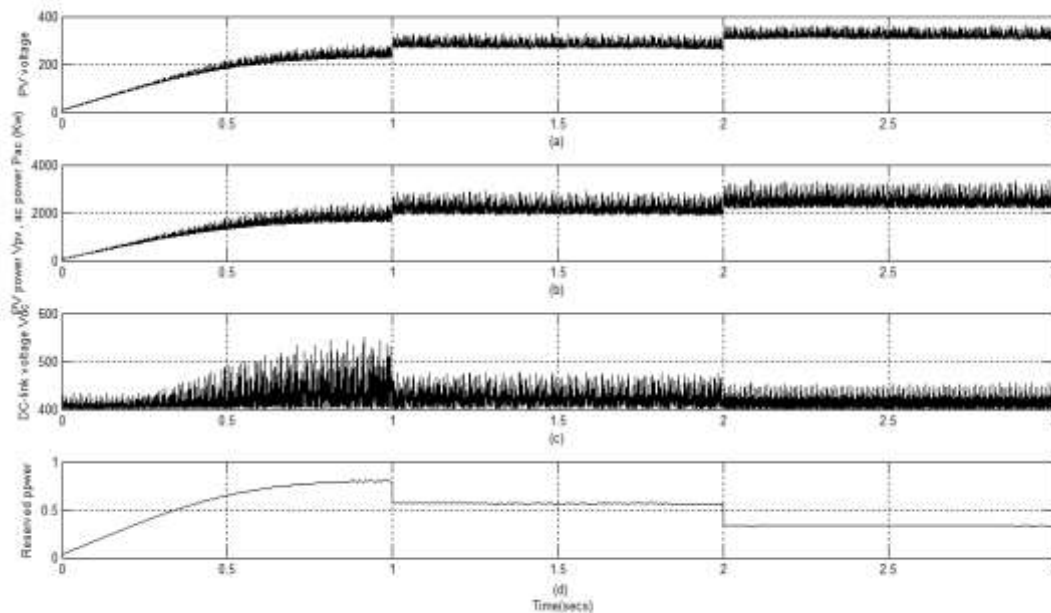


Fig. 5 Results of the single-phase grid-connected PV system with the proposed RPC strategy during the steady-state operation

The Fig. 5 represents a constant solar irradiance profile of 1000 W/m^2 , corresponding to the available PV power of 3 KW has been adopted in the test. In this case, three reserve power references ΔP 700, 500, and 300 W are used to verify the effectiveness of the RPC strategy during steady-state operation, the results are shown in Fig.5. The PV voltage V_{pv} and the corresponding extracted PV power P_{pv} are shown in Fig. 5(a) and (b), respectively. During the CPG operation periods, the extracted PV power P_{pv} is limited below the available power P_{avail} corresponding to the amount of the reserve power ΔP , while the PV power reaches the available power during the MPPT mode. At the grid side, the average injected ac power $\langle P_{ac} \rangle$ always follows the RPC constraint during operation, as it can be seen in Fig. 5(a). This is achieved by the stored energy controller, where the DC-link voltage v_{dc} is adaptively controlled to absorb the peak power injection in the DC link during the MPPT mode. It can be noticed in Fig. 5(c) that the variation in the DC link voltage increases as the amount of reserve power increases, while the average value remains the same. More specifically, the DC-link voltage only increases temporarily during the APE process in order to store the excess energy in the DC-link. In this case, the peak DC-link voltage is highest when the reserve power is 700W, as it can be seen from Fig. 5. This is in a close agreement with the previous theoretical analysis according to Control of a PV generator to maintain active reserve power during operation. Nevertheless, the average reserved power ΔP can be accurately controlled according to the references, as it is shown in Fig. 5(d).

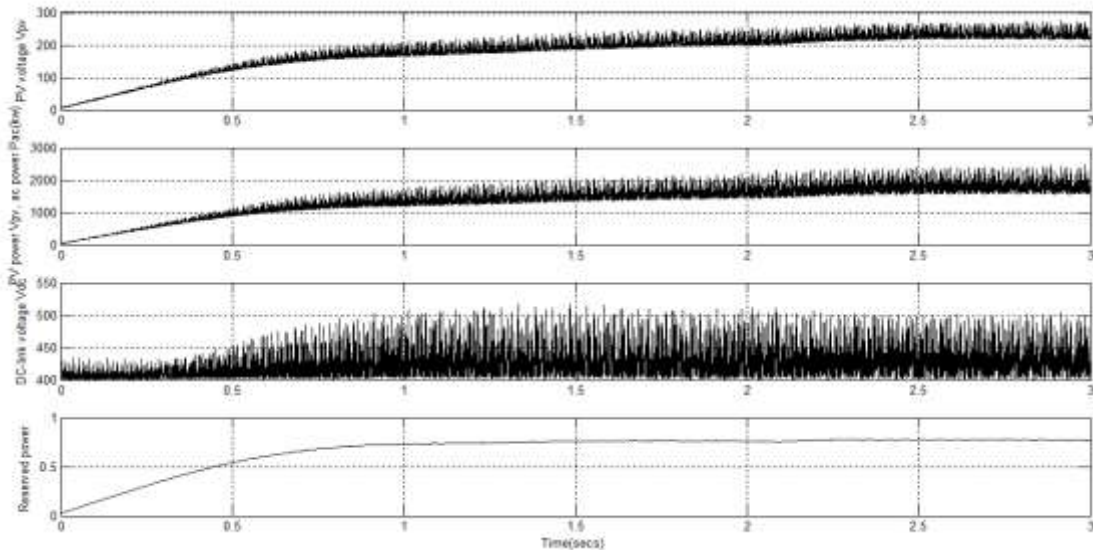


Fig. 6 Results of the single-phase grid-connected PV system with the proposed

RPC strategy at the sampling rate of $f_{APE} = 0.05$ Hz under a ramp-changing solar irradiance profile

The Fig. 6 represents the proposed RPC strategy has also been verified with a ramp-changing irradiance profile, where the performance of the APE process becomes important. As mentioned previously, the accuracy of the APE process relies on its sampling rate f_{APE} . Thus, two different sampling frequencies of $f_{APE} = 0.05$ and 0.2 Hz are used in this test, while the reference reserve power ΔP is kept as 500 W. The performances of the RPC with a low sampling frequency of the APE process are shown in Fig. 6. The PV voltage v_{pv} under this operating condition is shown in Fig. 6(a), where it can be seen that the MPPT operation is assigned to the boost converter every 20 s, $f_{APE} = 0.05$ Hz. In Fig. 6(b), the available PV power P_{avai} and the extracted PV power P_{pv} during operation are shown, which demonstrates that the available power P_{avai} is periodically measured in the MPPT mode. The injected ac power (P_{ac}) during operation is also shown in the same figure, where it can be observed that the reserve power constraint is achieved. However, a reserve power profile ΔP in Fig. 6(d), presents a considerable error during operation due to the low sampling rate of the APE process.

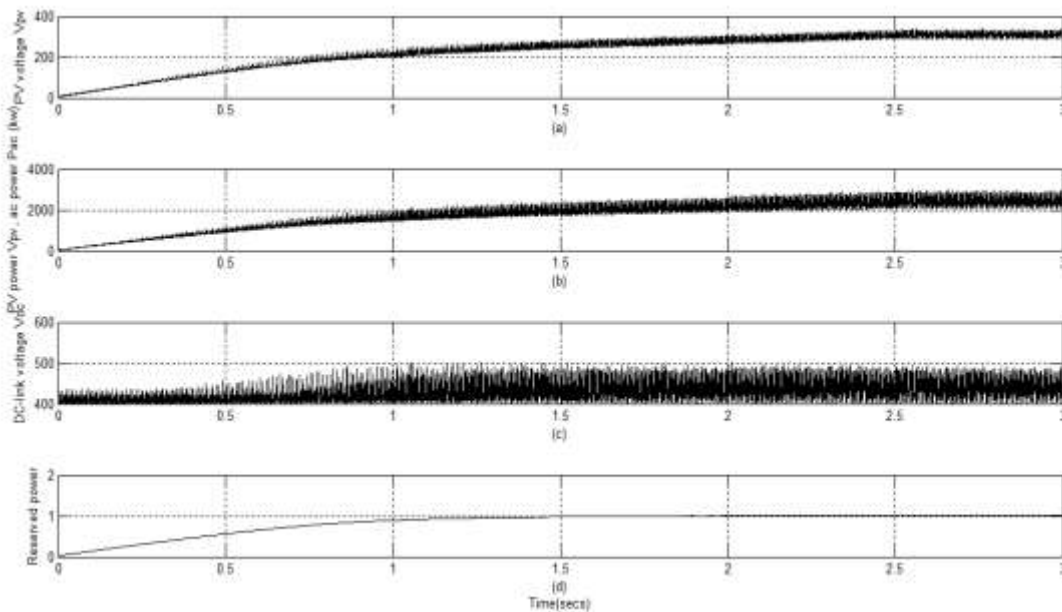


Fig. 7 The Results of the single-phase grid-connected PV system with the proposed RPC strategy at the sampling rate of $f_{APE} = 0.2$ Hz under a ramp-changing solar irradiance profile

The Fig. 7 represents in order to reduce the reserve power error and demonstrate the impact of the sampling frequency of the APE process f_{APE} on the performance of the RPC strategy, a high sampling rate of 0.2 Hz for the APE process is adopted in Fig. 7. In this case, the MPPT operation is assigned to the boost converter every 5 s, $f_{APE} = 0.2$ Hz. This can be noticed from the PV voltage v_{pv} in Fig. 7(a), where the CV-MPPT algorithm is assigned more frequently compared to that in Fig. 7(a). A similar high frequency transition between the MPPT and CPG mode is also observed in the extracted PV power P_{pv} in Fig. 7(b). On the other hand, the injected ac power (P_{ac}) fluctuation is reduced with this high sampling rate due to the higher accuracy in the APE. Consequently, the error in the reserved power ΔP is significantly reduced, as it can be seen from Fig. 7(d).

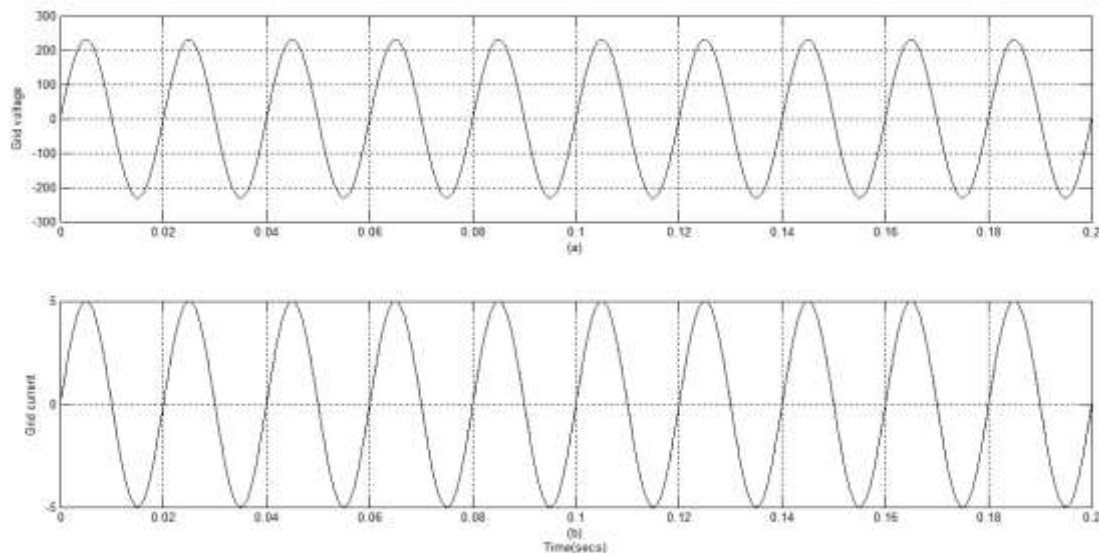


Fig. 8 Grid voltage & grid current

The Fig. 8 represents grid voltage and grid current, the grid connected voltage is 230V and grid connected current is 5A, the power is 1150W.

CONCLUSION:

The cost-effective reserve power control strategy for two-stage grid-connected PV systems to be applied, which is achieved by routinely employing a fast MPPT operation. Then, the estimated available power is used for calculating the set point to limit the extracted PV power with the CPG operation. At the grid side, the stored energy in the DC link is adaptively controlled to minimize the power fluctuation during the available PV power estimation process, where the excess energy is temporarily stored in the DC link. With the aforementioned coordinated control strategy, the reserve power control can be achieved.

REFERENCES:

- [1] *Technische Richtlinie Erzeugungsanlagen am Mittelspannungsnetz— Richtlinie für Anschluss und Parallelbetrieb von Erzeugungsanlagen am Mittelspannungsnetz*, BDEW, Berlin, Germany, Jun. 2008.
- [2] Energinet. dk, “Technical regulation 3.2.2 for PV power plants with a power output above 11 kW,” Tech. Rep. Doc. 14/17997-39, 2015.
- [3] E. Troester, “New German grid codes for connecting PV systems to the medium voltage power grid,” in *Proc. 2nd Int. Workshop Concentrating Photovolt. Power Plants: Opt. Design, Prod., Grid Connection*, pp. 1–4, 2009.
- [4] B. I. Craciun, T. Kerekes, D. Sera, and R. Teodorescu, “Frequency support functions in large PV power plants with active power reserves,” *IEEE J. Emerg. Sel. Topics Power Electron.*, vol. 2, no. 4, pp. 849–858, Dec. 2014.
- [5] A. Hoke, E. Muljadi, and D. Maksimovic, “Real-time photovoltaic plant maximum power point estimation for use in grid frequency stabilization,” in *Proc. IEEE 16th Control Model. Power Electron.*, pp. 1–7, Jul. 2015.
- [6] REN21, “Renewables 2016: Global status report (GRS),” 2016. [Online]. Available: <http://www.ren21.net/>
- [7] Fraunhofer ISE, “Recent facts about photovoltaics in germany,” Apr. 22, 2016. [Online]. Available: <http://www.pv-fakten.de/>
- [8] Solar Power Europe, “Global market outlook for solar power 2015–2019,” 2015. [Online]. Available: <http://www.solarpowereurope.org/>
- [9] E. Reiter, K. Ardani, R. Margolis, and R. Edge, “Industry perspectives on advanced inverters for us solar photovoltaic systems: Grid benefits, deployment challenges, and emerging solutions,” National Renewable Energy Laboratory (NREL), Tech. Rep. no. NREL/TP-7A40-65063, 2015.
- [10] Y. Yang, P. Enjeti, F. Blaabjerg, and H. Wang, “Wide-scale adoption of photovoltaic energy: Grid code modifications are explored in the distribution grid,” *IEEE Ind. Appl. Mag.*, vol. 21, no. 5, pp. 21–31, Sep. 2015.
- [11] E. Romero-Cadaval, B. Francois, M. Malinowski, and Q. C. Zhong, “Grid-connected photovoltaic plants: An alternative energy source, replacing conventional sources,” *IEEE Ind. Electron. Mag.*, vol. 9, no. 1, pp. 18–32, Mar. 2015.
- [12] A. Sangwongwanich, Y. Yang, F. Blaabjerg, and H. Wang, “Benchmarking of constant power generation strategies for single-phase grid-connected photovoltaic systems,” in *Proc. Appl. Power Electron. Conf.*, pp. 370–377, Mar. 2016.
- [13] A. Sangwongwanich, Y. Yang, and F. Blaabjerg, “High-performance constant power generation in grid-connected PV systems,” *IEEE Trans. Power Electron.*, vol. 31, no. 3, pp. 1822–1825, Mar. 2016.
- [14] L. D. Watson and J. W. Kimball, “Frequency regulation of a microgrid using solar power,” in *Proc. Appl. Power Electron. Conf.*, pp. 321–326, Mar. 2011.

- [15] S. Mishra, P. P. Zarina, and P. C. Sekhar, "A novel controller for frequency regulation in a hybrid system with high PV penetration," in *Proc. IEEE Power Energy Soc. Gen. Meeting*, pp. 1–5, Jul. 2013.
- [16] B. I. Craciun, T. Kerekes, D. Sera, and R. Teodorescu, "Frequency support functions in large PV power plants with active power reserves," *IEEE J. Emerg. Sel. Topics Power Electron.*, vol. 2, no. 4, pp. 849–858, Dec. 2014.
- [17] S. Nanou, A. Papakonstantinou, and S. Papathanassiou, "Control of a PV generator to maintain active power reserves during operation," in *Proc. Eur. Photovolt. Sol. Energy Conf. Exhib.*, pp. 4059–4063, 2012.
- [18] N. Kakimoto, S. Takayama, H. Satoh, and K. Nakamura, "Power modulation of photovoltaic generator for frequency control of power system," *IEEE Trans. Energy Convers.*, vol. 24, no. 4, pp. 943–949, Dec. 2009.
- [19] H. Beltran, E. Bilbao, E. Belenguer, I. Etxeberria-Otadui, and P. Rodriguez, "Evaluation of storage energy requirements for constant production in PV power plants," *IEEE Trans. Ind. Electron.*, vol. 60, no. 3, pp. 1225–1234, Mar. 2013.
- [20] H. Beltran, E. Bilbao, E. Belenguer, I. Etxeberria-Otadui, and P. Rodriguez, "Evaluation of storage energy requirements for constant production in PV power plants," *IEEE Trans. Ind. Electron.*, vol. 60, no. 3, pp. 1225–1234, Mar. 2013.
- [21] N. A. Rahim, R. Saidur, K. H. Solangi, M. Othman, and N. Amin, "Survey of grid-connected photovoltaic inverters and related systems," *Clean Technol. Environ. Policy*, vol. 14, no. 4, pp. 521–533, 2012.
- [22] Y. Yang and F. Blaabjerg, "Overview of single-phase grid-connected photovoltaic systems," *Elect. Power Compon. Syst.*, vol. 43, no. 12, pp. 1352–1363, 2015.
- [23] F. Blaabjerg, R. Teodorescu, M. Liserre, and A. V. Timbus, "Overview of control and grid synchronization for distributed power generation systems," *IEEE Trans. Ind. Electron.*, vol. 53, no. 5, pp. 1398–1409, Oct. 2006.
- [24] R. Gonzalez, J. Lopez, P. Sanchis, and L. Marroyo, "Transformer less inverter for single-phase photovoltaic systems," *IEEE Trans. Power Electron.*, vol. 22, no. 2, pp. 693–697, Mar. 2007.
- [25] T. Esram and P. L. Chapman, "Comparison of photovoltaic array maximum power point tracking techniques," *IEEE Trans. Energy Convers.*, vol. 22, no. 2, pp. 439–449, Jun. 2007.
- [26] Y. Yang, H. Wang, F. Blaabjerg, and T. Kerekes, "A hybrid power control concept for PV inverters with reduced thermal loading," *IEEE Trans. Power Electron.*, vol. 29, no. 12, pp. 6271–6275, Dec. 2014.
- [27] D. Premm, B. Osterkamp, J. Seidel, S. Poehling, A. Unru, and B. Engel, "The PV-Regel project—Development of concepts and solutions for the provision of control reserve with PV," in *Proc. Eur. Photovolt. Sol. Energy Conf. Exhib.*, pp. 3124–3128, 2015.
- [28] H. Xin, Z. Lu, Y. Liu, and D. Gan, "A center-free control strategy for the coordination of multiple photovoltaic generators," *IEEE Trans. Smart Grid.*, vol. 5, no. 3, pp. 1262–1269, May 2014.
- [29] A. Sangwongwanich, Y. Yang, and F. Blaabjerg, "Sensorless reserved power control strategy for two-stage grid-connected photovoltaic systems," in *Proc. IEEE 7th Int. Symp. Power Electron. Distrib. Gener. Syst.*, pp. 1–8, Jun. 2016.
- [30] Y. T. Tan, "Impact on the power system with a large penetration of photovoltaic generation," Ph.D. dissertation, Dept. Elect. Eng. Electron., Univ. Manchester Inst. Sci. Technol., Manchester, U.K., Feb. 2004.
- [31] European Network of Transmission System Operators for Electricity, "Network code for requirements for grid connection applicable to all generators," Technical Report, Mar. 2013. [Online]. Available: [https:// www.entsoe.eu.2013](https://www.entsoe.eu.2013) European Network of Transmission System Operators for Electricity, "Network code for requirements for grid connection applicable to all generators," Technical Report, Mar. 2013. [Online]. Available: [https:// www.entsoe.eu.2013](https://www.entsoe.eu.2013)
- [32] *National Electrical Code: 2008*. National Fire Protection Association, Quincy, MA, USA, 2007.
- [33] *IEC 61730: Photovoltaic (PV) Module Safety Qualification.*, International Electrotechnical Commission, IEC 61730, 2016.
- [34] H. Wang and F. Blaabjerg, "Reliability of capacitors for dc-link applications in power electronic converters—An overview," *IEEE Trans. Ind. Appl.*, vol. 50, no. 5, pp. 3569–3578, Sep. 2014.
- [35] N. Mohan, T. M. Undeland, and W. P. Robbins, *Power Electronics: Converters, Applications, and Design*. New York, NY, USA: Wiley, 2003.